Nanowires Grown on InP (100): Growth Directions, Facets, Crystal Structures, and Relative Yield Control

H. Aruni Fonseka,[†,*] Philippe Caroff,[†] Jennifer Wong-Leung,[†,‡] Amira S. Ameruddin,[†,§] Hark Hoe Tan,[†] and Chennupati Jagadish[†,*]

[†]Department of Electronic Materials Engineering, Research School of Physics and Engineering, The Australian National University, Canberra, ACT 0200, Australia, [‡]Centre for Advanced Microscopy, The Australian National University, Canberra, ACT 0200, Australia, and [§]Faculty of Science, Technology and Human Development, Universiti Tun Hussein Onn Malaysia, Parit Raja, 86400, Batu Pahat, Johor, Malaysia

ABSTRACT Growth of III–V nanowires on the [100]-oriented industry standard substrates is critical for future integrated nanowire device development. Here we present an in-depth analysis of the seemingly complex ensembles of epitaxial nanowires grown on InP (100) substrates. The nanowires are categorized into three types as vertical, nonvertical, and planar, and the growth directions, facets, and crystal structure of each type are investigated. The nonvertical growth directions are mathematically modeled using a three-dimensional multiple-order twinning concept. The nonvertical nanowires can be further classified into two different types, with one type growing in the ⟨111⟩ directions and the other in the ⟨100⟩ directions after initial multiple three-dimensional twinning. We find that 99% of the total nanowires are grown either along ⟨100⟩, ⟨111⟩, or ⟨110⟩ growth directions by {100} or {111} growth facets. We also demonstrate relative control of yield of these different types of nanowires, by tuning pregrowth annealing conditions and growth parameters. Together, the knowledge and controllability of the types of nanowires provide an ideal foundation to explore novel geometries that combine different crystal structures, with potential for both fundamental science research and device applications.

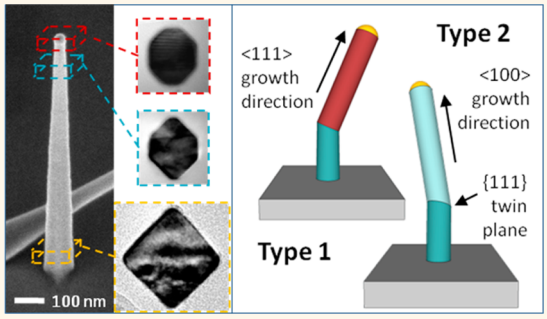

KEYWORDS: (100) substrates · InP nanowires · ⟨100⟩-oriented nanowires · 3D twinning · planar nanowires · pregrowth anneal

Since the first observation of catalyzed whisker growth by Wagner and Ellis,[1] semiconductor nanowires have been extensively grown and studied on surfaces with various crystal orientations. Among these, for cubic semiconducting materials the (111) surface is far more commonly used, due to the lower surface free energy of this surface, which promotes easy formation of vertical nanowires.[2−5] Unfortunately, owing to the stacking sequence of face centered cubic materials in the ⟨111⟩ direction, these vertical nanowires grown on (111) substrates are highly prone to stacking faults. This problem is very much prominent in InP, which has the lowest stacking fault energy out of the common cubic III–V semiconductors,[6,7] making the realization of pure crystal phase nanowires difficult and, in particular, achieving defect-free zincblende (ZB) ⟨111⟩ nanowires almost impossible. Vertical nanowires grown on (100) substrates, that is, nanowires adopting the [100] crystal orientation, have a major advantage of being twin or stacking fault free, despite the difficulty in achieving growth in this energetically unfavorable direction. Hence, it provides an opportunity to grow planar-defect-free ZB InP nanowires. Furthermore, (100) is the standard substrate orientation used in industry, and the ability to grow vertical nanowires on (100) substrates would enable seamless integration of InP nanowire devices with other planar electronic and photonic devices on a single chip.

A number of groups have grown III–V nanowires on (100) substrates.[8−21] It is seen that there is a considerable yield of nonvertical nanowires growing in various directions, unless the nanowire nucleation is tightly controlled.[8] The knowledge of these other growth directions and the properties of such nanowires are important in maximizing one growth direction over the other, and particularly in maximizing the vertical yield. Nevertheless, extensive studies have

* Address correspondence to axf109@physics.anu.edu.au, cxj109@physics.anu.edu.au.

Received for review March 31, 2014 and accepted June 2, 2014.

Published online June 02, 2014
10.1021/nn5017428

not been carried out to this effect. Also, the existence and control of different growth orientations on the same substrate could provide options for creating new structures and unique devices such as nanocrosses, zigzag bioprobes, and light-harvesting geometries, as demonstrated in recent reports.[8,13,14,21−25]

In the current study, we present an in-depth analysis into the seemingly complex growth directions of the InP nanowires that are grown on InP (100) substrates. Three main types of nanowires, namely, vertical, nonvertical, and planar, are identified to be growing on the (100) substrates. In addition to growth directions, the side facets, growth facet, and crystal structure of each of these types are investigated in detail. A mathematical model based on the three-dimensional (3D) twinning concept[26] is presented to explain the nonvertical nanowire growth directions, and the model is verified by the experimental results. It is shown that 99% of the nanowires grown on InP (100) substrates grow along either the ⟨100⟩, ⟨111⟩, or ⟨110⟩ direction driven by either a {100} or {111} growth facet, which is not perpendicular to the growth direction in the case of planar nanowires. We also demonstrate the relative yield control of each of these types of nanowires by varying the pregrowth conditions and growth parameters.

RESULTS AND DISCUSSION

Figure 1a shows a scanning electron microscopy (SEM) image of a typical nanowire sample catalyzed by colloidal Au particles. Three main types of nanowires can be identified: (1) vertical nanowires (indicated by blue arrows), (2) nonvertical nanowires that grow at an inclined angle with respect to the substrate surface (yellow arrows), and (3) planar nanowires that grow along the substrate (red arrows). It is worth investigating these three types of nanowires that grow on (100) substrates in detail. In the following section, growth directions, facets, and the crystal structure of each of these types of nanowires will be discussed. For in-depth analysis of the types of nanowires, a sample consisting of 83% vertical nanowires, 7% nonvertical nanowires, and 10% planar nanowires was selected as the principal sample. However, other samples with different relative yields (as specified when required) were also considered in order to obtain an overall understanding.

First, let us consider the vertical nanowires grown on the InP (100) substrates.

Vertical Nanowires. Figure 1b and c show 45° tilted and top views of vertical nanowires of the principal sample that was grown at 450 °C, respectively. The side facets of the vertical nanowires can be {100}, {110}, or a combination of the two (resulting in an octagonal cross-section) depending on the growth condition and the particle size. The type of side facets is independent of the pregrowth annealing condition. Here, they broadly appear to be of {100} type for the nanowires grown at 450 °C, as seen in Figure 1c. Figure 1d shows a

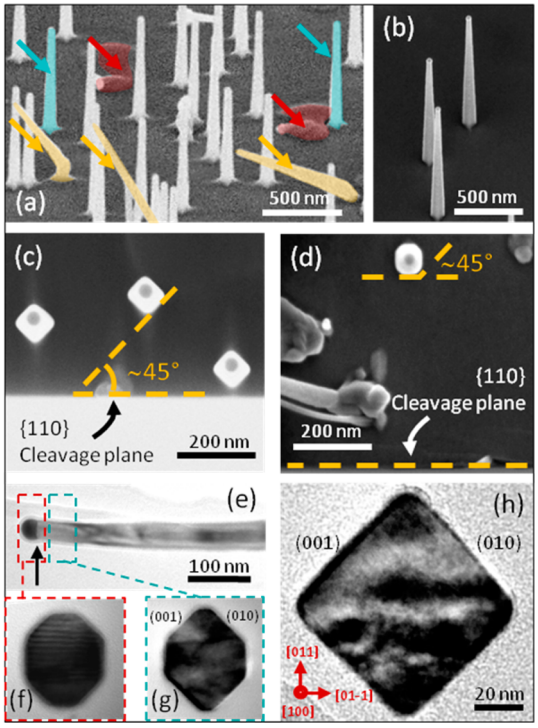

Figure 1. (a) SEM 45° tilted view of the three main types of nanowires grown on InP (100) substrates: vertical nanowires in blue, nonvertical nanowires in yellow, and planar nanowires in red. (b) SEM 45° tilted view of the vertical nanowires. (c) Top view of vertical nanowires with {100} sides facets, shown with respect to the {110} cleavage plane. (d) Top view of a vertical nanowire from a growth that gives a combination of {110} and {100} side facets. (e) TEM image of a nanowire from the sample shown in (b) and (c), indicating the regions where cross-sections (f) and (g) were obtained. The black arrow indicates the (100) growth facet. (f−h) X-TEM images of slices taken from the (f) topmost region, (g) region just below the particle, and (h) bottom region of vertical nanowires from the sample shown in (b) and (c). (e) is imaged along the ⟨011⟩ zone axis, while (f)−(h) cross-sections are imaged along the ⟨100⟩ zone axis. Images (f)−(h) are of the same magnification.

vertical nanowire from a sample grown at 425 °C showing an octagonal cross-sectional shape with {110} and {100} side facets. Cross-sectional transmission electron microscopy (X-TEM) analysis was carried out in order to ascertain the side facet evolution along the vertical nanowires shown in Figure 1b and c. The TEM images of the cross sections taken across the topmost area with the Au particle, the area just below the particle, and the bottom of the nanowires are shown in Figure 1f, g, and h, respectively. The cross-section TEM image of the topmost area indicates that the growth facet just below the Au particle is of octagonal shape. The octagon comprises of four {100} facets and four {110} facets. In this case, the lateral growth of the {110} facets is faster compared to the {100} facets, and a square cross-section comprising {100} facets is formed toward the bottom of the nanowire as a result of lateral growth.

Yet, as seen in Figure 1g, the lateral growth of the two types of {110} facets that are orthogonal to each other does not take place at the same rate. (011) and

(0−1−1) facets grow faster than (01−1) and (0−11) side facets. {011} planes are nonpolar, meaning they have an equal number of group III and V atoms terminating the surface. However, in order to explain the above anisotropy, one has to consider the two orthogonal (011) and (01−1) planes with a slight angle toward the top of the nanowire, as it would be in a tapered nanowire. As shown in the Supporting Information Figure S1, although the {011} planes are nonpolar on their own, the step structure formed by an incline would show a partial polarity with uneven numbers of group III and V atoms on the surface. This partial polarity is group III rich (A-polar) for (011) and (0−1−1) facets and group V rich (B-polar) for (01−1) and (0−11) facets. Under group V rich, high V/III ratio growth conditions similar to those used in our study, the growth of "A"-type facets takes place much faster than "B"-type facets.[27−29] Hence, during the lateral growth and tapering of the nanowire, the (011) and (0−1−1) side facets grow faster than (01−1) and (0−11) side facets, resulting in an elongated octagonal shape cross-section toward the top-mid area of the nanowire, as seen in Figure 1g.

The growth facet of these vertical nanowires is the (100) facet that is parallel to the substrate (as indicated by the black arrow in Figure 1e), and it should be noted that it is not a combination of {111} lower energy facets as seen in some ⟨100⟩ nanowires.[4] The crystal structure of the vertical nanowires is defect-free ZB, in agreement with the previous reports.[8−11,30]

Next, the nonvertical nanowires are discussed and their growth directions are derived using a 3D multiple-order twinning model.

Nonvertical Nanowires. As seen in Figure S2 of the Supporting Information, the nonvertical nanowires that grow inclined to the surface may initially seem randomly oriented. However, close inspection reveals that a vast majority of these nonvertical nanowires can be broadly divided into two major subtypes, differentiated by their morphology and dimensions: type 1, less tapered longer nanowires (Figure 2a), and type 2, more tapered shorter nanowires (Figure 2b) whose morphology is similar to vertical [100] nanowires.

We show that these are ⟨111⟩ and ⟨100⟩ nanowires, respectively, which acquire nonvertical growth directions due to the 3D twinning that takes place at the bottom of the nanowire. The two types are illustrated in Figure 2c, with extended vertical segments for clarity. The two types are characterized in detail in the following subsections.

Type 1. Most of the nanowires with type 1 morphology grow along the two directions that are parallel to the (011) cleavage plane and make a 35° angle with the substrate surface. From crystallography, it can be easily concluded that these are nanowires that grow in two of the four ⟨111⟩ directions that project out of the (100) substrate. Yet, there is a minority of nanowires that do not fit the direct ⟨111⟩ growth directions when considering the angles they create with the surface and the cleavage plane.

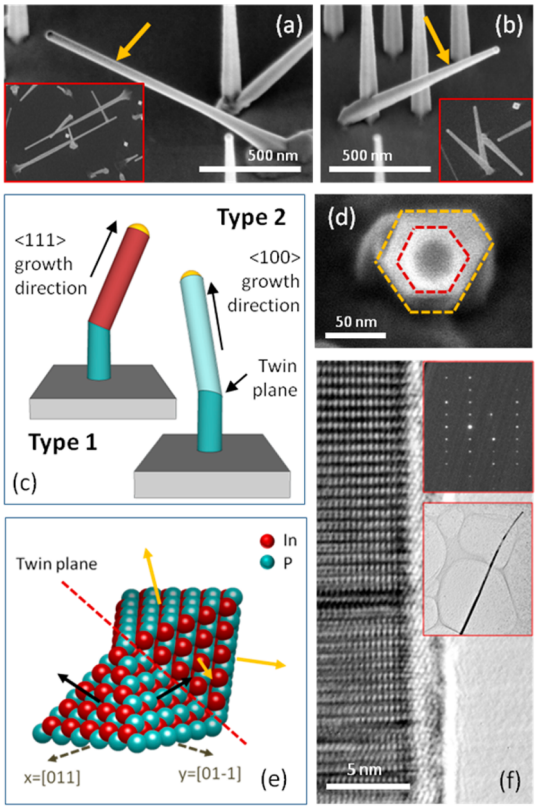

Figure 2. (a) SEM image of a nonvertical nanowire with a less tapered and long morphology, with the inset showing the top view of two similar nanowires. (b) A nonvertical nanowire with a more tapered morphology, similar to vertical nanowires, with the inset showing the top view of similar nanowires. (c) The two types of nonvertical nanowires, illustrated with extended untwinned [100] vertical segments for clarity. (d) A first-order ⟨111⟩ nonvertical nanowire viewed along its growth axis, showing the {1−100} ({112} ZB equivalent) side facets. (e) An atomistic model showing the possible first- and second-order twinned ⟨111⟩ growth directions; black solid arrows showing first-order growth directions from the untwinned primary crystal and yellow solid arrows showing the second-order ⟨111⟩ directions from the twinned crystal. (f) High-resolution TEM image showing the defective WZ crystal structure of a ⟨111⟩ nonvertical nanowire, and the insets show the diffraction pattern from the ⟨11−20⟩ zone axis and the low-magnification image of the same nanowire.

Uccelli *et al.* have shown that the unusual nonvertical growth directions seen in self-catalyzed GaAs nanowires grown on Si (111) can be explained by 3D multiple-order twinning of the seed particle.[26] Here we have extended this model for nanowires growing along the ⟨111⟩ directions after twinning on {111} planes on the (100) substrate, by transforming the axis system to suit the (100) substrate. The atomistic model in Figure 2e shows the untwinned {111} half-octahedron and one possible three-dimensionally twinned octahedron with respect to the (100) substrate. Black and yellow arrows indicate the possible direct ⟨111⟩ growth directions and ⟨111⟩ growth directions after

one 3D twin, respectively. The derivation of the model and the theoretical calculation of expected angles are given in the Supporting Information Sections 1 and 2.

Table S1 in the Supporting Information Section 3 summarizes all the possible growth directions of twinned ⟨111⟩ nanowires up to the third order, where the number of possible growth directions increases exponentially with the order of twinning. These expected growth directions are experimentally corroborated by the angles measured of the nonvertical nanowires in our principal sample. The projection angle measurements were taken on individual nanowires with respect to the cleavage planes and substrate normal by rotating and tilting in the SEM. The experimental frequency of occurrence as a percentage of the total type 1 nonvertical nanowires is given in the last column of Table S1. The frequency of occurrence decreases with the order of twinning. It should also be noted that all ⟨111⟩ nanowires measured in the current study are of B polarity, meaning they only grow along the ⟨111⟩ B directions.

Nanowires grown in the ⟨111⟩ directions generally have a significantly higher growth rate compared to those grown in the ⟨100⟩ direction, similar to the reference nanowires grown on InP (111)B substrates in the same growth run. Figure 2d shows a first-order ⟨111⟩ nanowire imaged 35° tilted to the {110} cleavage plane, so that the electron beam is parallel to the nanowire axis. As shown in this figure, the side facets form a hexagonal shape with a hexagonal or truncated triangular tapered bottom that is typically seen for nanowires grown on (111) substrates. By considering the interplanar angles the nanowire facets make with the substrate and the {110} cleavage plane, they are derived to be {112} facets. This is also similar to the reference nanowires grown on InP (111)B substrate under the same growth conditions, which show {112}-type side facets.

Once growth in the ⟨111⟩ direction is initiated, it is comparable to the growth on (111) substrates. Twin planar defects perpendicular to the growth direction can now be easily created, and hexagonal wurtzite (WZ) phase can also form depending on the growth conditions. As shown in Supporting Information Section 5, this is due to the fact that in ⟨111⟩ directional growth, each new layer can nucleate in a ZB or WZ position, independent of the previous stacking sequence (given the formation energy requirement is satisfied).[31] Figure 2f shows a TEM image of a ⟨111⟩ nanowire grown on an InP (100) substrate. As the growth orientation information is lost during the sample preparation process for TEM analysis, they are initially identified as ⟨111⟩-oriented nanowires by matching the morphology. This is later verified by indexing the diffraction patterns. The nonvertical nanowires grown along ⟨111⟩ directions are of WZ crystal phase with some stacking faults, again, similar to those grown vertically on InP (111)B substrates under the same growth conditions. Hence, the actual facets of the nanowires are of {1−100} type, which is the equivalent of ZB {112} planes in the WZ phase.

⟨111⟩ nanowires are the most commonly reported type of nonvertical nanowires that grow on (100) substrates.[9,14−19] However, in our case we find that, depending on the growth conditions, up to about 60% of the nonvertical nanowire growth directions could not be explained by direct or multiple-order twinned ⟨111⟩ growth directions, that is by the "type 1" scenario. By inspecting the morphology, one could also see that these unexplained nanowires are generally of the above-mentioned type 2.

Type 2. Here, the 3D multiple order twinning takes place on {111} planes, similarly to the previous case. However, after twinning, the nanowires grow in ⟨100⟩ directions instead. This scenario can be visualized as shown in the atomistic model in Figure 3a, where three possible ⟨100⟩ directions (indicated by yellow arrows) are available for growth from the resulting twinned crystal. Figure 3b and c show a 3D-computer model and a SEM image of a second-order type 2 nanowire viewed at the same tilt angle with respect to the substrate. The {111} planes are shown in the model for clarity and comparison. The existence of the twin plane can be identified in the SEM image due to the difference in lateral overgrowth at the twin plane.

The possible growth directions with respect to the substrate can be calculated using the same model used before, by substituting the relevant ⟨100⟩ growth direction instead of the ⟨111⟩ direction. The model and derivation of growth directions are given in the Supporting Information Sections 1 and 2. Table S2 in the Supporting Information Section 4 shows all possible growth directions for 3D multiple-order twinned ⟨100⟩ nanowires up to the third order. Experimentally measured angles of the individual type 2 nonvertical nanowires confirm the presented model. The relative frequency of occurrence of type 2 nonvertical nanowires with the order of twinning is given in Table S2.

The morphology and growth rate of nonvertical ⟨100⟩ nanowires are similar to the vertical [100] nanowires. The inset of Figure 3d shows the same second-order, type 2 nonvertical nanowire shown in Figure 3d, but imaged 72° rotated from the (011) cleavage edge and 48° tilted to the vertical so that the electron beam is parallel to the nanowire axis. The facets of the nanowire can be derived to be {100} by considering the twinned crystal orientation. This is similar to what was seen for the vertical nanowires in the same sample. The side facets of the type 2 nonvertical nanowires were also examined in the samples in which the vertical nanowires showed octagonal cross-sections (combination of {100} and {110}) similar to Figure 1d. It is seen that the side facets of these type 2 nonvertical nanowires are also octagonal and similar to the vertical

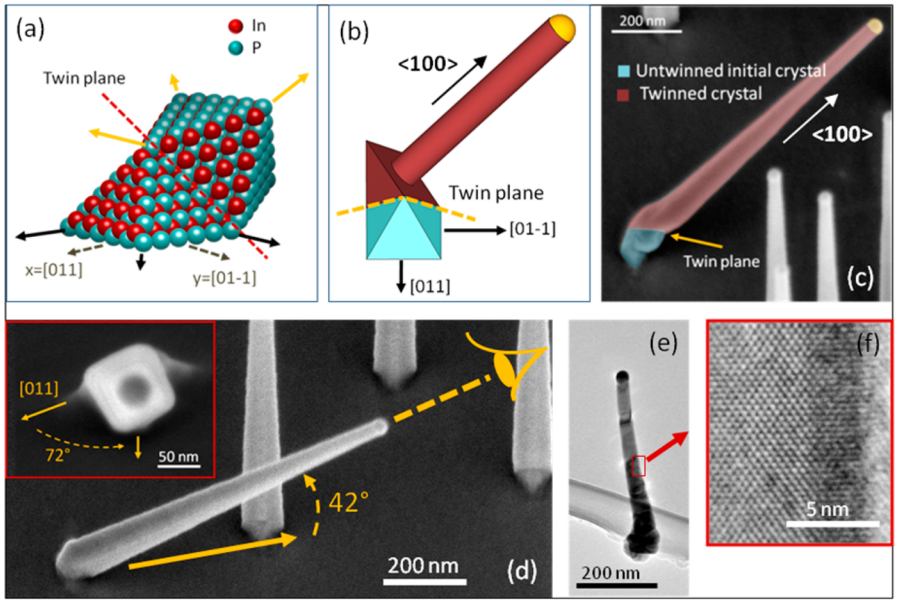

Figure 3. (a) An atomistic model showing the first- and second-order nonvertical ⟨100⟩ growth directions; first-order directions are shown by black solid arrows from the untwinned primary crystal and second-order ⟨100⟩ directions by yellow solid arrows from the twinned crystal. (b, c) A 3D model (b) and an SEM image (c) of a second-order nonvertical type 2 nanowire making α and $\varphi_{[011]}$ angles of 42° and 108°, viewed along the same direction and tilt for comparison. The half {111} octahedra of the initial and twinned crystals are shown for ease of comparison with the atomistic model in (a) and for an understanding of the evolution of nanowire growth direction by twin formation. (d) Second-order type 2 ⟨100⟩ nanowire showing the viewing direction for the image shown in the inset. (e) Low-magnification TEM micrograph of a nonvertical ⟨100⟩ nanowire with the twinned bottom region. (f) HRTEM image showing the ZB crystal structure above the twinned base.

nanowires of the same sample. Therefore, it can be concluded that the side facets of all ⟨100⟩ nanowires are the same for a particular growth condition and are not affected by the 3D twinning at the bottom of the nanowire.

As the morphology of the vertical and nonvertical ⟨100⟩ nanowires are similar and the orientation information is lost in the transfer process to the Cu grid for TEM analysis, it is hard to be certain about the type of ⟨100⟩ nanowires that were analyzed under the TEM. However, while most nonvertical nanowires could break above the twinned bottom region, there are few nanowires similar to the one shown in Figure 3e that have broken off below the twinned section. These nanowires can be established to be nonvertical ⟨100⟩ nanowires. The crystal structure of these nanowires is also defect-free ZB once the growth in the ⟨100⟩ direction is initiated after the initial 3D twinning at the bottom.

For the principal sample considered, a total of 85% of the nonvertical nanowire growth directions matches with the above type 1 or type 2 multiple-order twinned directions considered up to the third order. It should be noted that the remaining 15% of nonvertical nanowires represents only 1% of the entire principal sample when considered with the other main types of nanowires. It should also be noted that the proportions of type 1 and type 2 nonvertical nanowires and even the distribution within the orders of the same type vary with the growth conditions.

Next, let us consider the planar nanowires, the third main type of nanowires grown on the (100) substrate.

Planar Nanowires. Planar nanowires were studied across a number of samples, including the principal sample. For X-TEM studies, a sample with 100% planar nanowires was used due to the ease of sample preparation and analysis.

The planar nanowires grow along the four in-plane ⟨110⟩ directions of the (100) substrate. As seen in Figure 4a, the tapering and the growth rate of the planar nanowires grown along the two perpendicular [011] (or [0−1−1]) and [01−1] (or [0−11]) directions are significantly different. Nanowires grown parallel to the [01−1] direction (indicated in blue in Figure 4a) are highly tapered and have a "Christmas tree"-like shape. The growth rate of these nanowires are also lower compared to those grown parallel to the [011] direction. The planar nanowires grown parallel to the [011] direction (indicated in red in Figure 4a) are nontapered. These nanowires also seem to show preference in growing along the [01−1] and [0−11] directions compared to the [011] and [0−1−1] directions. Interestingly, they can also change growth direction from one ⟨110⟩ direction to another by making 90° or 180° turns, as indicated by the arrows in Figure 4b and c. A close investigation of the facets of these nanowires helps in explaining the morphology and the behavior observed.

Figure 4d shows an X-TEM image of a planar nanowire taken along the ⟨011⟩ zone axis. As can be

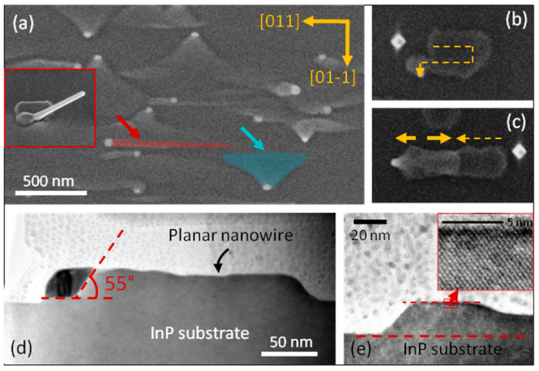

Figure 4. (a) SEM top view of the 100% planar nanowire sample, with a nanowire growing in the [011] direction indicated in red and a nanowire growing in the [01−1] direction indicated in blue. The in-set shows a planar nanowire from a different sample that has later grown off the surface as a nonvertical nanowire. (b) A planar nanowire making 90° turns and changing growth directions. (c) A planar nanowire that had made 180° turns and changed growth direction. (d) TEM micrograph showing the longitudinal cross-section of a planar nanowire from the same sample as in (a). (e) TEM micrograph showing the transverse cross-section of a planar nanowire with the inset showing the ZB crystal structure.

clearly seen, the predominant growth facet of the nanowire is a {111} plane, although the resultant growth direction is ⟨110⟩. This is similar to what has been previously observed for GaAs and InAs planar nanowires grown on (100) substrates.[20,21] Therefore, in the case of planar nanowires, the growth direction is not perpendicular to the growth facet. Growth on the other facet revealed by the Au particle, *i.e.*, the (100) facet, is very slow compared to that on the {111} plane. The base of the planar nanowires (*i.e.*, the parts that grew first) is gradually submerged with time in the two-dimensional layer growth that simultaneously takes place on the substrate, creating an illusion as if the bottoms of these nanowires are thinner than the tip. As seen in Figure 4e, the planar nanowires maintain the (100) top facet.

The growth of the nanowire being driven by a {111} plane explains the preference of these nanowires to grow along the [01−1] and [0−11] directions compared to the [011] and [0−1−1] directions. Nanowires grown along the [01−1] and [0−11] directions are driven by (111)B polar growth facets, while those grown along the [011] and [0−1−1] directions are driven by (111)A polar growth facets. In the case of nanowires grown on (111) substrates, it is known that they generally prefer to grow along the ⟨111⟩B direction (that is, driven by a (111)B facet) than along the ⟨111⟩A direction (driven by a (111)A facet).[32,33] Similarly in this case, [01−1] (and [0−11]) oriented planar nanowires that have the (111)B facets as growth facets are dominant. However, it should be noted that the presence of some planar nanowires driven by (111)A growth facets is in contrast to what has been reported for GaAs and InAs planar nanowires,[20,21] where all nanowires were aligned parallel to [01−1], *i.e.*, driven by (111)B facets. A similar alignment parallel to [01−1] has been observed for self-catalyzed InP planar nanowires, although the exact growth facet is not clear in this case.[33] In the current study, the (111) facet that is driving the growth of the planar nanowire can even switch between the four available {111} facets on the (100) surface, causing them to change growth direction in 90° and 180° angles. The cause of growth direction change is not completely clear. However, from careful examination of the SEM images it is clear that the presence of obstacles such as other nanowires (planar, vertical, and nonvertical) and uneven depositions on the substrate is one definite cause. As seen in the inset of Figure 4a, few planar nanowires may end up growing as nonvertical or even vertical nanowires, growing off the substrate during the later stage of growth.

The fact that the nanowires parallel to the [011] direction are grown by a (111)A facet also explains their faster axial growth rate. In the case of ⟨111⟩ nanowires, it has been reported that the ⟨111⟩A nanowires have a higher growth rate than the ⟨111⟩B nanowires.[16] Similarly in this case, the planar nanowires that are driven by (111)A facets grow faster axially. The difference in tapering and lateral growth of the two perpendicular types of nanowires could be resulting from a combination of two mechanisms. First, it has been shown that the relative lateral growth rates in the two perpendicular [011] and [01−1] directions depend on the metal organic vapor phase epitaxy (MOVPE) growth conditions.[34] At relatively low temperatures and high V/III ratios the lateral growth rate in the [011] direction is faster than in the [01−1] direction due to the ease of group III adatom incorporation on the group V covered [011] steps.[34] This higher lateral growth rate in the [011] direction results in higher tapering of the nanowires growing perpendicular to the [011] direction, that is, parallel to the [01−1] direction. The second mechanism involves the side facets of the planar nanowires that are shown in Figure 4e. These facets that are sloping from the top facet to the substrate are partially or fully polar, similar to those discussed in the vertical nanowires section. For planar nanowires grown parallel to [01−1], the polarity of the side facets is "A", while for nanowires grown parallel to [011] the polarity of the side facets is "B". As discussed earlier, with the higher growth rate of A polar facets under the considered growth conditions,[27−29] the side facets of the [01−1] and [0−11] planar nanowires grow faster, making them more tapered and giving them the "Christmas tree"-like shape.

As seen in the TEM micrographs of Figure 4d and e, the planar nanowires have a defect-free ZB crystal structure, in agreement with GaAs and InAs[20,21] planar nanowires. Despite being mainly grown by a {111} facet, the planar nanowires tend to be twin-defect-free ZB due to the fact that they grow along the substrate

TABLE 1. Summary of Growth Directions, Facets, and Crystal Structure of Nanowires Grown on InP (100) Substrates

	NW type	growth direction	NW side facets	growth facet	crystal structure
1	vertical	[100]	{100}, {110}, or combination of the two	(100)	planar-defect-free ZB
2	nonvertical	⟨111⟩ after 3D multiple-order twinning at the bottom	{112}/{1−100} (same as the facets of NWs grown on (111) substrate under the same conditions)	{111}	WZ with some stacking faults
		⟨100⟩ after 3D multiple-order twinning at the bottom	{100}, {110}, or combination (same as vertical [100] NWs on the same substrate)	{100}	planar-defect-free ZB
3	planar	four ⟨110⟩ directions	(100) top facet, side facets are nonuniform	{111}	planar-defect-free ZB

and hence directly epitaxial to the substrate along the whole length of the nanowire. This prohibits the nucleus from taking WZ positions, unlike in the case of ⟨111⟩-oriented nanowires (see Supporting Information Section 5).

Table 1 summarizes the growth directions, facets, and crystal structure of the three types of nanowires (NW) discussed above.

Ninety-nine percent of the nanowires on the principal sample can be explained by the three main types given in Table 1. Hence, considering the growth facets of these types of nanowires, it can be concluded that a vast majority of seemingly complicated nanowires grown on InP (100) substrates are actually driven by only two kinds of facets: {111} and {100}. It should also be noted that nonvertical nanowire growth directions such as ⟨110⟩ and ⟨112⟩, which are commonly seen on (111) and (100) substrates,[11,35−38] are not observed in this case.

Relative Yield Control of the Three Types of Nanowires. All three types of nanowires discussed above have been successfully demonstrated in devices, and one type or the other may be preferred depending on the application and device design.[13,14,21−25] Yet, for device purposes the relative control of growth of one type over another is paramount in order to minimize device fabrication complexities as well as to increase efficiency. In this section, we present the relative yield control of the types of nanowires discussed above, by tuning the pregrowth conditions and the growth parameters.

Vertical. Vertical growth of nanowires is highly sensitive to the pregrowth annealing condition of the Au catalyst particles as well as the growth parameters of the nanowires. We find that nanowire growth in this otherwise energetically unfavorable direction does not allow for a large growth parameter window. Pregrowth annealing under a relatively low temperature and a low phosphine (PH_3) flow promotes subsequent vertical growth of nanowires. Growth temperatures between 450 and 475 °C and V/III ratios in the range of 350 are favorable for vertical nanowires. The trimethylindium (TMIn) precursor flow rate should also be low, in the region of 2.015×10^{-6} mol/min. Eighty-five percent vertical nanowires are achieved by pregrowth annealing at 390 °C under a PH_3 flow of 8.93×10^{-4} mol/min and then carrying out the growth at 450 °C and a V/III ratio of 350.

It has also been shown in the recent reports by Wang *et al.*[8,10] that the pregrowth conditioning of the particles as well as growth conditions play a critical role in achieving very high vertical yield. In this technique the Au particles are prefilled with In prior to growth instead of annealing. The nanowire growth temperature and the V/III ratio used are comparable, while the TMIn molar fraction is higher.

Nonvertical. Nonvertical nanowire growth mainly depends on the flow rate of TMIn during the nanowire growth. Sixty-seven percent nonvertical nanowires are achieved by using a high flow rate of TMIn, at 4.030×10^{-5} mol/min, for the same pregrowth annealing condition used for the vertical nanowires above. The growth temperature and the V/III ratio are maintained at 450 °C and 350, respectively.

Planar. Planar nanowire growth is highly sensitive to the pregrowth annealing condition. High pregrowth annealing temperature and high PH_3 flow during annealing promote formation of planar nanowires. One-hundred percent planar nanowires can be achieved for the same nanowire growth condition as the above vertical nanowires by simply annealing the sample at 600 °C under high PH_3 flow of 2.23×10^{-3} mol/min.

The pregrowth annealing and growth conditions for high yields of each type of nanowires are summarized in Table 2.

In order to gain insight into the effect of growth conditions on the type of nanowires grown, we have studied the initial stages of formation of the three different types of nanowires. For the vertical and planar nanowires, the growth was carried out for a few seconds. In the case of nonvertical nanowires, a sample in which the nanowire growth direction changed (kinked) by forming 3D twins during the cooling down stage was used due to the ease of analysis.

The evolution of the three types of nanowires from nucleation to early growth stages is shown in a series of X-TEM images in the Supporting Information Figure S5. Comparing the particles that have only been annealed, it is clear that the different pregrowth annealing treatment has affected the nanoparticle differently (see Figure S5(a)i and (b)i). The particle collects In from the substrate and forms an alloy during the pregrowth annealing. Comparing the sizes of the particles along the evolution, it is also clear that the particle absorbs more In during the initial stages of growth.

TABLE 2. Summary of Pregrowth Annealing Conditions and Growth Parameters to Achieve High Yields of Different Types of Nanowires

		pregrowth annealing condition		growth parameters			
	NW type	temperature	PH_3 flow (mol/min)	temperature	V/III	TMIn flow (mol/min)	yield (%)
1	vertical	390 °C	8.93×10^{-4}	450 °C	350	2.015×10^{-6}	85
2	nonvertical	390 °C	8.93×10^{-4}	450 °C	350	4.030×10^{-5}	67
3	planar	600 °C	2.23×10^{-3}	450 °C	350	2.015×10^{-6}	100

Hence, as Wang *et al.*[8] have shown, the In percentage in the particle could be playing a role in determining the growth direction. Yet, it should be noted that pregrowth annealing at lower temperature (390 °C), which should incorporate less In, has resulted in higher vertical yield in our case. This observation is not in complete agreement with ref 8, where a relatively high In concentration had led to a high vertical yield.

Careful examination of the nanoparticle−substrate/nanowire interface during the early stages of growth (see three series (a−c) in Supporting Information Figure S5) also reveals that the facets that are wetted by the Au particle are dynamically changing before selection of the final growth direction. In most cases, the particle wets multiple facets that are in competition before the final growth direction is established. Theoretical models by Schwarz and Tersoff[39,40] have shown that the different growth directions may arise from interplay between facet growth and introduction of new facets at the growth front as well as droplet statics. They have also shown that different growth modes can be stable under the same growth conditions, and the actual growth mode is decided by the initial conditions such as annealing and patterning,[40] which is similar to our case of planar and vertical nanowire growth. This is due to the new facets formation during the complex transient state before a steady state is established,[40,41] which is also evident in our experimental results.

Although the kinked nanowires used for this study (Supporting Information Figure S5 series c) do not directly correspond to the growth conditions used for the sample with a high nonvertical yield in Table 2, they give an understanding of the process of 3D twin formation and changes in the position of the nanoparticle that vary with the external In supply. Group III flow (or group III partial pressure) has been shown to affect the surface energies as well as chemical potential of the nanoparticle.[39,42] In the current study, the growth is further complicated by the presence of multiple growth facets in the initial stage of growth, which could eventually lead to tilting and 3D twin formation. More detailed quantitative modeling of the complex initial conditions, which is beyond the scope of this paper, is required in order to fully understand the effect of these pregrowth annealing and growth conditions on the resulting nanowire type.

CONCLUSION

The nanowires grown on InP (100) substrates are identified to be of three main types: vertical, nonvertical, and planar nanowires. These types of nanowires are analyzed in detail in terms of morphology, growth directions, facets, and crystal structure. Two kinds of nonvertical nanowires are found, and a mathematical model based on 3D multiple-order twinning is presented to explain the growth directions of these two kinds of nonvertical nanowires. The experimental data obtained by measuring elevation and azimuth angles of the individual nanowires confirm the calculated values using the model. We find that the seemingly complex and random nanowire growth on InP (100) substrates simplifies to nanowires driven by either {100} or {111} growth facets. ⟨110⟩ and ⟨112⟩ growth directions that are commonly seen on (111) and (100) substrates are not observed in this case. Finally, the relative yield control of these different types of nanowires by tuning the pregrowth annealing conditions and growth parameters is demonstrated. A low pregrowth annealing temperature and precursor flow are preferred by vertical nanowires, while nonvertical nanowires prefer a high precursor flow rate. Planar nanowires are achieved by increasing the pregrowth annealing temperature and PH_3 flow during this step. An in-depth understanding of these different types of nanowires and the ability to control their relative growth would increase the usability of the nanowires grown on the industry standard (100)-oriented substrates in a wide range of device applications.

EXPERIMENTAL METHODS

All samples were prepared immediately prior to growth by dispersing 30 nm colloidal Au particles on poly-L-lysine-coated (100) InP substrates. A (111)B InP substrate prepared using the same method was also included in each growth run as a reference. Nanowires were grown in a horizontal flow MOVPE reactor with a total flow of 15 slm, using TMIn and PH_3 as In and P sources, respectively. The samples were annealed for 10 min under PH_3 flow in order to enhance alloying between the substrate and the Au particle before initiating nanowire growth. The exact pregrowth annealing and growth conditions favoring

each of the types of nanowires are as given in Table 2. Nanowires were investigated using SEM and TEM. Cross-section TEM (X-TEM) samples of the planar nanowires, Au particles, and nanowires in the initial stages of growth were prepared by tripod polishing followed by ion beam polishing. Lateral cross-sections of the vertical nanowires were prepared by embedding the samples in a resin, followed by microtome sectioning.

Conflict of Interest: The authors declare no competing financial interest.

Supporting Information Available: Schematic showing formation of partially polar surfaces on tapered {011} nanowire facets (Figure S1), top view SEM image of a typical nanowire sample showing seemingly random nonvertical growth directions (Figure S2), growth direction calculation for 3D multiple-order twinned nanowires (Section 1), elevation and azimuth angle calculations for nonvertical nanowires (Section 2), 3D twinned growth directions of ⟨111⟩ nonvertical nanowires (Section 3), 3D twinned growth directions of ⟨100⟩ nonvertical nanowires (Section 4), growth orientation and crystal structure of ⟨111⟩, ⟨100⟩, and planar nanowires (Section 5), evolution of planar, vertical, and nonvertical nanowires (Figure S5). This material is available free of charge *via* the Internet at http://pubs.acs.org.

Acknowledgment. The Australian Research Council is acknowledged for the financial support, and the Australian National Fabrication Facility and the Australian Microscopy and Microanalysis Research Facility are acknowledged for providing access to the equipment used.

REFERENCES AND NOTES

1. Wagner, R. S.; Ellis, W. C. Vapor-Liquid-Solid Mechanism of Single Crystal Growth. *Appl. Phys. Lett.* **1964**, *4*, 89–90.
2. Braun, W.; Kaganer, V. M.; Trampert, A.; Schönherr, H.-P.; Gong, Q.; Nötzel, R.; Däweritz, L.; Ploog, K. H. Diffusion and Incorporation: Shape Evolution during Overgrowth on Structured Substrates. *J. Cryst. Growth* **2001**, *227−228*, 51–55.
3. Fortuna, S. A.; Li, X. Metal-Catalyzed Semiconductor Nanowires: A Review on the Control of Growth Directions. *Semicond. Sci. Technol.* **2010**, *25*, 024005.
4. Wang, N.; Cai, Y.; Zhang, R. Q. Growth of Nanowires. *Mater. Sci. Eng., R* **2008**, *60*, 1–51.
5. Stekolnikov, A. A.; Furthmüller, J.; Bechstedt, F. Absolute Surface Energies of Group-IV Semiconductors: Dependence on Orientation and Reconstruction. *Phys. Rev. B* **2002**, *65*, 115318.
6. Gottschalk, H.; Patzer, G.; Alexander, H. Stacking Fault Energy and Ionicity of Cubic III−V Compounds. *Phys. Status Solidi A* **1978**, *45*, 207–217.
7. Oda, O.; Fukui, T.; Uchida, R.; Kohiro, K.; Kurita, H.; Kainosho, K.; Asahi, S.; Suzuki, K. *InP and Related Compounds: Materials, Applications and Devices*; Manasreh, M. O., Ed.; Gordon and Breach Science Publishers, 2000; pp 17−18.
8. Wang, J.; Plissard, S. R.; Verheijen, M. A.; Feiner, L.-F.; Cavalli, A.; Bakkers, E. P. A. M. Reversible Switching of InP Nanowire Growth Direction by Catalyst Engineering. *Nano Lett.* **2013**, *13*, 3802–3806.
9. Krishnamachari, U.; Borgstrom, M.; Ohlsson, B. J.; Panev, N.; Samuelson, L.; Seifert, W.; Larsson, M. W.; Wallenberg, L. R. Defect-Free InP Nanowires Grown in [001] Direction on InP (001). *Appl. Phys. Lett.* **2004**, *85*, 2077–2079.
10. Wang, J.; Plissard, S.; Hocevar, M.; Vu, T. T. T.; Zehender, T.; Immink, G. G. W.; Verheijen, M. A.; Haverkort, J.; Bakkers, E. P. A. M. Position-Controlled [100] InP Nanowire Arrays. *Appl. Phys. Lett.* **2012**, *100*, 053107.
11. Li, Z.-A.; Möller, C.; Migunov, V.; Spasova, M.; Farle, M.; Lysov, A.; Gutsche, C.; Regolin, I.; Prost, W.; Tegude, F.-J.; *et al*. Planar-Defect Characteristics and Cross-Sections of ⟨001⟩, ⟨111⟩, and ⟨112⟩ InAs Nanowires. *J. Appl. Phys.* **2011**, *109*, 114320.
12. Seifert, W.; Borgström, M.; Deppert, K.; Dick, K. A.; Johansson, J.; Larsson, M. W.; Mårtensson, T.; Sköld, N.; Patrik, T.; Svensson, C.; Wacaser, B. A.; *et al*. Growth of One-Dimensional Nanostructures in MOVPE. *J. Cryst. Growth* **2004**, *272*, 211–220.
13. Muskens, O. L.; Diedenhofen, S. L.; Kaas, B. C.; Algra, R. E.; Bakkers, E. P. A. M.; Gómez Rivas, J.; Lagendijk, A. Large Photonic Strength of Highly Tunable Resonant Nanowire Materials. *Nano Lett.* **2009**, *9*, 930–934.
14. Kang, J.-H.; Cohen, Y.; Ronen, Y.; Heiblum, M.; Buczko, R.; Kacman, P.; Popovitz-Biro, R.; Shtrikman, H. Crystal Structure and Transport in Merged InAs Nanowires MBE Grown on (001) InAs. *Nano Lett.* **2013**, *13*, 5190–5196.
15. Ambrosini, S.; Fanetti, M.; Grillo, V.; Franciosi, A.; Rubini, S. Self-Catalyzed GaAs Nanowire Growth on Si-Treated GaAs(100) Substrates. *J. Appl. Phys.* **2011**, *109*, 094306.
16. Wacaser, B. A.; Deppert, K.; Karlsson, L. S.; Samuelson, L.; Seifert, W. Growth and Characterization of Defect Free GaAs Nanowires. *J. Cryst. Growth* **2006**, *287*, 504–508.
17. Murakami, S.; Funayama, H.; Shimomura, K.; Waho, T. Au-Assisted Growth of InAs Nanowires on GaAs(111)B, GaAs(100), InP(111)B, InP(100) by MOVPE. *Phys. Status Solidi C* **2013**, *10*, 761–764.
18. Hiruma, K.; Yazawa, M.; Katsuyama, T.; Ogawa, K.; Haraguchi, K.; Koguchi, M.; Kakibayashi, H. Growth and Optical Properties of Nanometer-Scale GaAs and InAs Whiskers. *J. Appl. Phys.* **1995**, *77*, 447–462.
19. Gao, L.; Woo, R. L.; Liang, B.; Pozuelo, M.; Prikhodko, S.; Jackson, M.; Goel, N.; Hudait, M. K.; Huffaker, D. L.; Goorsky, M. S.; *et al*. Self-Catalyzed Epitaxial Growth of Vertical Indium Phosphide Nanowires on Silicon. *Nano Lett.* **2009**, *9*, 2223–2228.
20. Zi, Y.; Jung, K.; Zakharov, D.; Yang, C. Understanding Self-Aligned Planar Growth of InAs Nanowires. *Nano Lett.* **2013**, *13*, 2786–2791.
21. Fortuna, S. A.; Wen, J.; Chun, I. S.; Li, X. Planar GaAs Nanowires on GaAs (100) Substrates: Self-Aligned, Nearly Twin-Defect Free, and Transfer-Printable. *Nano Lett.* **2008**, *8*, 4421–4427.
22. Strudley, T.; Zehender, T.; Blejean, C.; Bakkers, E. P. A. M.; Muskens, O. L. Mesoscopic Light Transport by Very Strong Collective Multiple Scattering in Nanowire Mats. *Nat. Photonics* **2013**, *7*, 413–418.
23. Xu, L.; Jiang, Z.; Qing, Q.; Mai, L.; Zhang, Q.; Lieber, C. M. Design and Synthesis of Diverse Functional Kinked Nanowire Structures for Nanoelectronic Bioprobes. *Nano Lett.* **2012**, *13*, 746–751.
24. Plissard, S. R.; van Weperen, I.; Car, D.; Verheijen, M. A.; Immink, G. W. G.; Kammhuber, J.; Cornelissen, L. J.; Szombati, D. B.; Geresdi, A.; Frolov, S. M.; *et al*. Formation and Electronic Properties of InSb Nanocrosses. *Nat. Nanotechnol.* **2013**, *8*, 859–864.
25. Miao, X.; Zhang, C.; Li, X. Monolithic Barrier-All-Around High Electron Mobility Transistor with Planar GaAs Nanowire Channel. *Nano Lett.* **2013**, *13*, 2548–2552.
26. Uccelli, E.; Arbiol, J.; Magen, C.; Krogstrup, P.; Russo-Averchi, E.; Heiss, M.; Mugny, G.; Morier-Genoud, F. o.; Nygård, J.; Morante, J. R.; *et al*. Three-Dimensional Multiple-Order Twinning of Self-Catalyzed GaAs Nanowires on Si Substrates. *Nano Lett.* **2011**, *11*, 3827–3832.
27. Kayser, O. Selective Growth of InP/GaInAs in LP-MOVPE and MOMBE/CBE. *J. Cryst. Growth* **1991**, *107*, 989–998.
28. Verheijen, M. A.; Algra, R. E.; Borgström, M. T.; Immink, G.; Sourty, E.; van Enckevort, W. J. P.; Vlieg, E.; Bakkers, E. P. A. M. Three-Dimensional Morphology of GaP−GaAs Nanowires Revealed by Transmission Electron Microscopy Tomography. *Nano Lett.* **2007**, *7*, 3051–3055.
29. Zou, J.; Paladugu, M.; Wang, H.; Auchterlonie, G. J.; Guo, Y.-N.; Kim, Y.; Gao, Q.; Joyce, H. J.; Tan, H. H.; Jagadish, C. Growth Mechanism of Truncated Triangular III−V Nanowires. *Small* **2007**, *3*, 389–393.
30. Björk, M. T.; Ohlsson, B. J.; Sass, T.; Persson, A. I.; Thelander, C.; Magnusson, M. H.; Deppert, K.; Wallenberg, L. R.; Samuelson, L. One-Dimensional Heterostructures in Semiconductor Nanowhiskers. *Appl. Phys. Lett.* **2002**, *80*, 1058–1060.
31. Glas, F.; Harmand, J.-C.; Patriarche, G. Why Does Wurtzite Form in Nanowires of III-V Zinc Blende Semiconductors? *Phys. Rev. Lett.* **2007**, *99*, 146101.
32. Fonseka, H. A.; Tan, H. H.; Wong-Leung, J.; Kang, J. H.; Parkinson, P.; Jagadish, C. High Vertical Yield InP Nanowire

Growth on Si(111) Using a Thin Buffer Layer. *Nanotechnology* **2013**, *24*, 465602.
33. Mattila, M.; Hakkarainen, T.; Jiang, H.; Kauppinen, E. I.; Lipsanen, H. Effect of Substrate Orientation on the Catalyst-Free Growth of InP Nanowires. *Nanotechnology* **2007**, *18*, 155301.
34. Asai, H. Anisotropic Lateral Growth in GaAs MOCVD Layers on (001) Substrates. *J. Cryst. Growth* **1987**, *80*, 425–433.
35. Adhikari, H.; Marshall, A. F.; Chidsey, C. E. D.; McIntyre, P. C. Germanium Nanowire Epitaxy: Shape and Orientation Control. *Nano Lett.* **2006**, *6*, 318–323.
36. Joyce, H. J.; Qiang, G.; Wong-Leung, J.; Kim, Y.; Tan, H. H.; Jagadish, C. Tailoring GaAs, InAs, and InGaAs Nanowires for Optoelectronic Device Applications. *IEEE J. Sel. Top. Quantum Electron.* **2011**, *17*, 766–778.
37. Cai, Y.; Chan, S. K.; Sou, I. K.; Chan, Y. F.; Su, D. S.; Wang, N. The Size-Dependent Growth Direction of ZnSe Nanowires. *Adv. Mater.* **2006**, *18*, 109–114.
38. Wu, Y.; Cui, Y.; Huynh, L.; Barrelet, C. J.; Bell, D. C.; Lieber, C. M. Controlled Growth and Structures of Molecular-Scale Silicon Nanowires. *Nano Lett.* **2004**, *4*, 433–436.
39. Schwarz, K. W.; Tersoff, J. Elementary Processes in Nanowire Growth. *Nano Lett.* **2010**, *11*, 316–320.
40. Schwarz, K. W.; Tersoff, J. Multiplicity of Steady Modes of Nanowire Growth. *Nano Lett.* **2012**, *12*, 1329–1332.
41. Schwarz, K. W.; Tersoff, J. From Droplets to Nanowires: Dynamics of Vapor-Liquid-Solid Growth. *Phys. Rev. Lett.* **2009**, *102*, 206101.
42. Algra, R. E.; Verheijen, M. A.; Feiner, L.-F.; Immink, G. G. W.; Enckevort, W. J. P. v.; Vlieg, E.; Bakkers, E. P. A. M. The Role of Surface Energies and Chemical Potential during Nanowire Growth. *Nano Lett.* **2011**, *11*, 1259–1264.